

# Leakage detection and location in gas pipelines through an LPV identification approach

P. Lopes dos Santos\* T-P Azevedo-Perdicoúlis\*\* G. Jank\*\*\*  
J. A. Ramos\*\*\*\* J. L. Martins de Carvalho†

\* *Faculdade de Engenharia da Universidade do Porto, Rua Dr Roberto Frias s/n, 4200-465 Porto, Portugal, (e-mail: pjsantos@fe.up.pt)*

\*\* *ISR—Coimbra & Departamento de Matemática, UTAD, 5001-801 Vila Real, Portugal, (e-mail: tazevedo@utad.pt)*

\*\*\* *RWTH-University of Technology, Department of Mathematics, 52056 Aachen, Germany, (e-mail: jank@math2.rwth-aachen.de)*

\*\*\*\* *Farquhar College of Arts and Sciences, Division of Mathematics, Science, and Technology, Nova Southeastern University, 3301 College Avenue, Fort Lauderdale, FL 33314, USA, (e-mail: jr1284@nova.edu)*

† *Faculdade de Engenharia da Universidade do Porto, Portugal, (e-mail: jmartins@fe.up.pt)*

---

**Abstract:** A new approach to gas leakage detection in high pressure distribution networks is proposed, where two leakage detectors are modelled as a Linear Parameter Varying (LPV) system whose scheduling signals are, respectively, intake and offtake pressures. Running the two detectors simultaneously allows for leakage location. First, the pipeline is identified from operational data, supplied by REN-Gasodutos and using an LPV systems identification algorithm proposed in [Lopes dos Santos et al., 2008b]. Each leakage detector uses two Kalman filters where the fault is viewed as an augmented state. The first filter estimates the flow using a calculated scheduling signal, assuming that there is no leakage. Therefore it works as a reference. The second one uses a measured scheduling signal and the augmented state is compared with the reference value. Whenever there is a significant difference, a leakage is detected. The effectiveness of this method is illustrated with an example where a mixture of real and simulated data is used.

Keywords: Gas Networks, Kalman Filter, Leakage Detection, LPV Subspace Identification.

---

## 1. INTRODUCTION

Leak detection and location is one of the paramount concerns of pipeline operators all over the world. A timely evaluation and response to a leak, allows proper management of the consequences and an effective risk minimisation. Present methods for gas leakage detection range from manual inspection using trained dogs to advanced satellite imaging [Geiger and Werner, 2003, Sivathanu, 2004, Zhang, 1996]. They can be classified as acoustic monitoring, optical monitoring, gas sampling, soil monitoring, flow monitoring and model-based methods. Flow monitoring and model based methods are widely used in the gas industry. Both continuously measure the pressure and/or massflow signals at different sections of the pipeline (mostly only at the extremes). Leaks are detected from the massflow balance equations, which consist in balancing the flow at the boundaries plus the variation of linepack (LP), i.e. the amount of gas stored in the pipes. However, a considerable drawback is the LP model being strongly dependent on the noise of the pressure/temperature measurements. In [Vostrý, 2004], corrections to the LP model in the pipelines are used to obtain a more robust method. Although in [Baptista et al., 2005] it is claimed that the

Simone<sup>®</sup> simulator allows for calculating accurately the LP, even under extreme conditions, these methods cannot be considered completely reliable since a significant number of false alarm rates is registered everyday. This is mainly due to an integral term of the balance equation, which integrates the massflow difference at the boundaries. These flow measurements are corrupted by noise which will be also integrated, introducing a random walk term in the balance equation. This term is a non-stationary stochastic process with a variance proportional to the integration time. As a result, the balance equation is always corrupted by a significant amount of noise that can easily trigger false alarms. Some model based methods avoid this problem by using state observers with the fault parameters treated as augmented states [Benkherouf and Allidina, 1988, Liu et al., 2005]. Although this is an appealing approach, the models used so far were too complex, giving rise to estimators with too high computational costs.

In [Lopes dos Santos et al., 2010], the pipeline is modelled as an LPV system and identified from operational data using an algorithm described in [Lopes dos Santos et al., 2007] and [Lopes dos Santos et al., 2008a]. The leakage is

detected with a Kalman filter where the fault is treated as an additional state.

In [Lopes dos Santos et al., 2011], the deduction of the LPV state space (SS) model structure with static and affine dependence on the scheduling signal shows that it is possible to represent the gas dynamics using a model of this type. Moreover, some of the parameters have no physical meaning and are not measurable. Therefore the need to use an identification algorithm.

Different algorithms exist for the problem of LPV state-space identification. Basically, we can distinguish between the subspace approaches and the ones based on the optimisation of a criterium. Usually, subspace methods are not iterative, but suffer from the curse of dimensionality even when dealing with low order models. The optimisation based models typically minimise quadratic error criteria. Since the error is not a linear function of the parameters, iterative algorithms are required and convergence to the global minima becomes an issue. We chose an iterative subspace method, whose algorithm guarantees convergence to a sub-optimal model under certain conditions. It also avoids the curse of dimensionality. Although, we cannot prove that the required convergence conditions are not fulfilled for this case, it has converged every time it has been run by the pipeline identification. Furthermore, the accuracy of the identified models showed to be always adequate for leakage detection. In the case of no suitability of the models, they can always be used as an initialisation to an optimisation procedure.

In [Lopes dos Santos et al., 2011] a new approach to gas leakage detection in high pressure natural gas transportation networks was proposed. The pipeline was modelled as an LPV system driven by the source node massflow with the LP as the scheduling parameter. The massflow at the offtake node is taken as the system output. The system is also identified by the algorithm described in [Lopes dos Santos et al., 2008b] and the leakage is detected using a Kalman filter where the fault is treated as an augmented state. Given that the gas LP can be estimated from the massflow balance equation, a differential method is proposed to improve the leakage detector effectiveness. The proposed LPV Kalman filter based methods were compared with a standard mass balance method in a simulated 10% leakage detection scenario. The Differential Kalman Filter method proved to be highly efficient.

In this paper the same approach is followed. Two leakage detectors are implemented, where the scheduling signal is first the intake pressure and next the offtake pressure. The pressures are calculated using an approximation of the lumped transfer function model for high pressure natural gas pipelines derived in [dos Santos et al., 2010a]; there, starting with a PDE model, a high order continuous state space linear model is obtained using a finite difference method. Next, from the SS representation an infinite order transfer function (TF) model is calculated. In the end, this TF is approximated by a compact non-rational function. This compact non-rational function may be further approximated by a simple integral model [dos Santos et al., 2010b].

In this article, in Section II the model is identified and the output is simulated using a Kalman filter. In Section

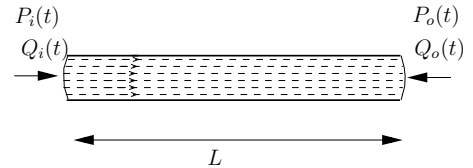
III, the two leakage detectors are described. Each leakage detector is essentially a Kalman filter with an additional state variable mimicking a leakage modelled as a random walk. In Section IV, an iterative leakage locator is deduced by comparison of the two leakage detectors. In Section V, we withdraw some conclusions and point out some directions along which we would like the work to proceed.

## 2. REPRESENTATION OF THE GAS DYNAMICS AS AN LPV MODEL

The gas dynamics in a pipeline may be represented by the following hyperbolic partial differential equations (Nieplocha:1):

$$\begin{cases} \frac{\partial Q(s,t)}{\partial t} = -S \frac{\partial P(s,t)}{\partial s} - \frac{\lambda c^2}{2dS} \frac{Q^2(s,t)}{P(s,t)} \\ \frac{\partial P(s,t)}{\partial t} = -\frac{c^2}{S} \frac{\partial Q(s,t)}{\partial s}, \end{cases} \quad (1)$$

where  $s$  is space,  $t$  is time,  $P$  is edge pressure-drop,  $Q$  is massflow,  $S$  is the cross-sectional area,  $d$  is the pipe diameter,  $c$  is the isothermal speed of sound, and  $\lambda$  is the friction factor. In the figure below,  $Q_i$  is the intake massflow and  $Q_o$  the offtake massflow and  $P_i$  is the intake pressure and  $P_o$  the offtake pressure. The time



pressure variations are assumed to have a unit correlation coefficient along the pipeline, and then are all proportional to a function  $\tilde{p}(t)$ , i.e.,  $\tilde{p}(s,t) = \mathbb{K}(s)\tilde{p}(t)$  [Lopes dos Santos et al., 2010]. Since the pressure varies slowly, this is a reasonable assumption for short length pipelines, i.e., ca. 35-50 Km. Under this assumption, a discrete LPV model with affine parameter dependence, with  $T_s$  as the sampling period, was obtained [Lopes dos Santos et al., 2010]. Hence:

$$\begin{aligned} x(k+1) &= A_0x(k) + A_p\tilde{p}(k)x(k) + B_0u(k) + B_p\tilde{p}(k)u(k) \\ y(k) &= C_0x(k) + C_p\tilde{p}(k)x(k) + D_0u(k) + D_p\tilde{p}(k)u(k). \end{aligned} \quad (2)$$

## 3. GAS PIPELINE LPV IDENTIFICATION

In this section, an LPV model was identified from a mixture of measured and simulated data of a gas pipeline depicted in the Figure 1 below:

Operational field measurements are all the intake/offtake massflows as well as the pressures along the entire network. These are available to Simone<sup>®</sup>, a simulator installed at REN-Gasodutos headquarters, through a SCADA system. Intermediate flow rate measurements are not available and need to be simulated. These are calculated by Simone<sup>®</sup> from the intake/offtake measured massflows. Simone<sup>®</sup> also computes the pressures along the network, which are compared with the measured ones to assess the simulator performance [GmbH and s.r.o, 2004, Wagner, 2004]. In our example, we used measured values for the pressures and for

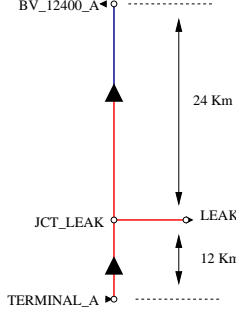


Fig. 1. Gas pipeline located in the South of Portugal, used as case study.

the intake massflow (a source point) and simulated values for the offtake flow. To simulate a leakage, we calculate the pressure drop, and then subtracted it from the measured pressure values.

For the case study, we consider a cylindrical pipeline with a diameter of  $d = 793$  mm, a length of  $L = 36$  Km, and a roughness factor of  $\lambda = 0.005$  mm. The TERMINAL\_A, JCT\_LEAK, and BV\_12400\_A are the pipeline intake node, the simulated leakage point, and the pipeline offtake node, respectively. The simulation reproduces a working gas day ( March, 2, 2009), in the closed interval  $[0h, 24h]$ , with no leakages, and at the constant temperature of  $18.5^\circ C$ . The data was collected with a sampling rate of 2 minutes.

Figure 2 depicts a working day data, i.e., the profiles of the intake and offtake pressure and massflow. We can see that the pressure time pattern seems to be the same for both endpoints of the pipeline. In fact it presents a correlation coefficient value of 0.9998, which validates the pressure proportionality assumption.

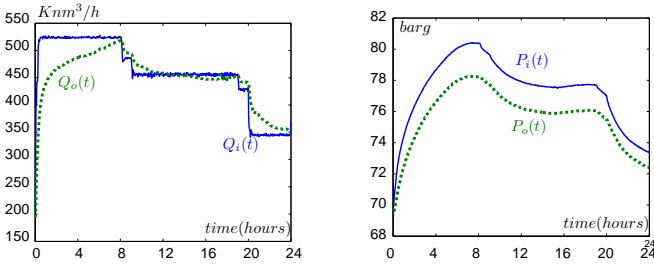


Fig. 2. Left: Intake and offtake massflows  $Q_i(t)$  (blue) and  $Q_o(t)$  (green). Right: Intake and offtake node pressures  $P_i(t)$  (blue) and  $P_o(t)$  (green).

For the first leakage detector the pipeline is modelled as the discrete LPV system, as in (2), using the time varying component (ac component) of the intake pressure as the scheduling signal. The second one uses the offtake pressure. The LPV models were identified with the Successive Approximations Subspace Identification Algorithm in [Lopes dos Santos et al., 2007] with the intake/offtake pressure as the scheduling parameter. These pressures were computed from:

$$P_{ic}(t) = \frac{K_G}{\alpha} Q_i(t) + K_G \int_{-\infty}^t Q_i(\tau) d\tau - \frac{K_G}{\alpha} Q_o(t)(t - T_L) - K_G \int_{-\infty}^t Q_o(\tau - T_L) d\tau \quad (3)$$

$$P_{oc}(t) = \frac{K_G}{\alpha} Q_i(t - T_L) + K_G \int_{-\infty}^t Q_i(\tau - T_L) d\tau - \frac{K_G}{\alpha} Q_o(t)(t) - K_G \int_{-\infty}^t Q_o(\tau) d\tau \quad (4)$$

with  $T_L = \frac{L}{c}$  and parameters  $K_G$ ,  $\alpha$  being estimated from the data. See [dos Santos et al., 2010b] for the derivation of the equations. Figure 3 compares the calculated with the

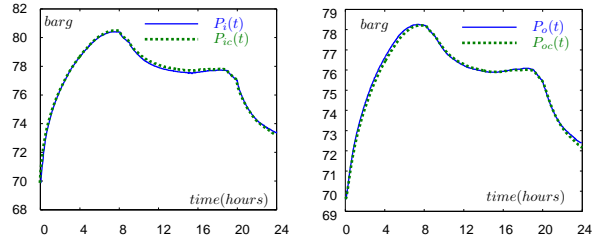


Fig. 3. Measured (blue) and calculated (green) pressures. Left: Intake node. Right: Offtake node.

measured values for both the intake and offtake pressures.

The LPV identification algorithm estimated two innovation models of the form:

$$\begin{aligned} x(k+1) &= A_0 x(k) + B_0 u(k) + A_p [\tilde{p}(k)x(k) \\ &\quad + B_p [\tilde{p}(k)u(k)] + K e(k) \\ y(k) &= C_0 x(k) + D_0 u(k) + C_p [\tilde{p}(k)x(k) \\ &\quad + D_p [\tilde{p}(k)u(k)] + e(k), \end{aligned} \quad (5)$$

with  $u(k) = Q_i(k)$ ,  $y(k) = Q_o(k)$  and  $\tilde{p}(k) = P_i(k) - \bar{P}_i$  or  $\tilde{p}(k) = P_o(k) - \bar{P}_o$ , where  $\bar{P}$  means the average value along time.  $e(k)$  is the zero mean white noise.

With the calculated intake pressure as the scheduling signal the following parameters were obtained:

$$\begin{aligned} A_{0i} &= 0.9661 B_{0i} = -0.1290 \times 10^{-1} C_{0i} = -2.0120, \\ D_{0i} &= 0.2101 B_{pi} = -0.5977 \times 10^{-3} A_{pi} = 0.3000 \times 10^{-2}, \\ C_{pi} &= 5.370, D_{pi} = -0.1340 \times 10^{-1} K_i = -0.1540. \end{aligned}$$

The left frame of Figure 4 compares the simulated offtake massflow with its true value. The right frame compares the predicted offtake massflow with its true value.

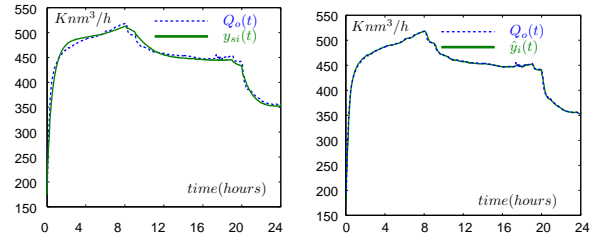


Fig. 4. Left: True  $Q_i(t)$ , (blue) and simulated  $y_{si}(t)$ , (green) offtake massflow. Right: True  $Q_i(t)$ , (blue) and predicted  $\hat{y}_i(t)$ , (green) offtake massflow.

When considering the calculated offtake pressure as the scheduling signal, the following parameters were obtained:

$$A_{0_o} = 0.9528, B_{0_o} = -0.191 \times 10^{-1}, C_{0_o} = -2.1137, \\ D_{0_o} = 0.1263, B_{p_o} = -0.6013 \times 10^{-3}, A_{p_o} = 0.2100 \times 10^{-2}, \\ C_{p_o} = 6.550, D_{p_o} = -0.393 \times 10^{-1}, K_o = -0.1570.$$

The left frame of Figure 5 compares the simulated and the predicted values with the true ones.

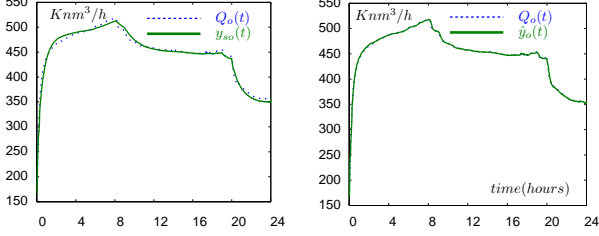


Fig. 5. Left: True  $Q_o(t)$ , (blue) and simulated  $y_{so}(t)$ , (red) offtake massflow. Right: True  $Q_o(t)$ , (blue) and predicted  $\hat{y}_o(t)$ , (red) offtake massflow.

#### 4. LEAKAGE DETECTION

In this section, a leakage was simulated by subtracting to the offtake massflow 10% from its mean value.

A method that uses a Kalman filter, built from an identified first order model, is described next. Thus, consider:

$$\begin{aligned} x_{leak_i}(k+1) &= x_{leak_i}(k) + e_{leak_i}(k) \\ x(k+1) &= A_0x(k) + B_0u(k) + A_p\tilde{p}(k)x(k) \\ &\quad + B_p\tilde{p}(k)u(k) + Ke(k) \\ y(k) &= x_{leak_i}(k) + C_0x(k) + D_0u(k) \\ &\quad + C_p\tilde{p}(k)x(k) + D_p\tilde{p}(k)u(k) + e(k), \end{aligned}$$

where  $A_0$ ,  $B_0$ ,  $C_0$ ,  $D_0$ ,  $A_p$ ,  $B_p$ ,  $C_p$ ,  $D_p$  are parameters of the identified model.  $e_{leak_i}(k)$  is also a zero mean white noise term, not correlated with  $e(k)$ , whose variance is a design parameter.  $x_{leak_i}(k)$  is the leakage detection signal and should be different from zero only in case of leakage.

This model has an additional state that is supposed to remain close to zero when there is no leakage. When a leakage occurs it should take the leakage value. From this idea, a Differential Kalman Filter based method was derived. This method consists in using two detectors and is identical to the one presented in [Lopes dos Santos et al., 2009], but the scheduling signals are now first the calculated intake pressure and second the calculated offtake pressure. The two different scheduling signals lead to two different leakage detectors, where each one runs two instances of this Kalman filter; the first instance uses the calculated pressure as the scheduling signal and the second uses the measured pressure. Since the first filter uses the calculated pressure it can never detect a leakage. Instead, it works as a reference signal. This filter leakage state is continuously compared with the corresponding state of the second filter, the one that uses the measured pressure as the scheduling signal. When there is no leakage, these states remain close to each other, but when a leakage occurs their difference takes the leakage value. In what follows, it can be seen, this method is very fast and accurate, and also well suited to detect small leakages.

We first describe the leakage detector whose scheduling signal is the intake pressure. The other leakage detector, i.e. the one that uses the offtake pressure as the scheduling signal is identical in every detail except for the chosen scheduling signal.

The calculated intake pressure,  $P_{ic}$ , is obtained from (3). Given that the leakage does not appear in this equation and the pressure solely depends on the intake/offtake massflows, the calculated scheduling signal always considers that there is no leakage in the pipeline. Thence, if we generate the scheduling parameter from this signal, a non leakage LPV model will always be identified and the Kalman filter should never detect a leakage. As a result, one should use this Kalman filter leakage estimate as a reference signal denoted by  $\hat{x}_{leak_i}^{ref}(k)$ . In parallel, one must run another instance of this Kalman filter using a scheduling signal generated from the measured intake pressure, i.e., from  $P_{im}(k)$ . This Kalman filter leakage estimate is denoted by  $\hat{x}_{leak_i}(k)$ . In the absence of leakage, both leakage estimates should be equal to zero. But, when a leakage occurs  $\hat{x}_{leak_i}^{ref}(k)$  remains zero and  $\hat{x}_{leak_i}(k)$  takes the value of the leakage. As such, the signal

$$\tilde{x}_{leak_i}(k) = \hat{x}_{leak_i}^{ref}(k) - \hat{x}_{leak_i}(k). \quad (6)$$

is leak sensitive and will be used to detect leakages. This signal depicted in Figure 6 represents a non faulty situation. It has an expected value of  $M_i = -0.1817 \text{ Knm}^3/h$

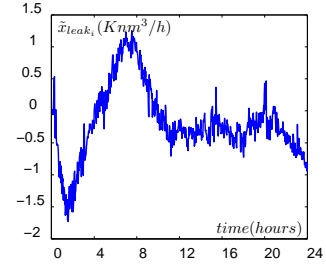


Fig. 6. Leak reference signal  $\tilde{x}_{leak_i}(k)$  in normal operation conditions (i.e. no leaks).

and a standard deviation  $\sigma_i = 0.5631 \text{ Knm}^3/h$ . From these values, upper and lower bounds of  $T_{Li}^{upper} = M_i + 3\sigma_i = 1.5075$  and  $T_{Li}^{lower} = M_i - 3\sigma_i = -1.8709$  were defined. A leakage is detected when this signal leaves the interval defined by these detection thresholds.

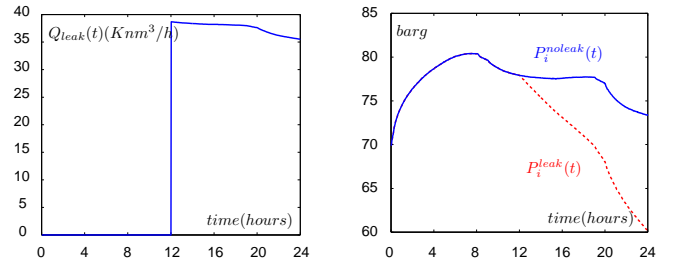


Fig. 7. Left: Leak massflow  $Q_{leak}$ . Right: Intake pressure drop due to leakage (red).

To illustrate this method, a leakage has been simulated at  $t = 12h$  and at the distance of 12 Km from the intake node. The left frame of Figure 7 shows the leakage massflow (ca. 10% massflow) and the right frame of Figure 7 shows the respective pressure reduction at the intake node of the

pipeline.  $\hat{x}_{leak_i}(k)$  was estimated for this leakage scenario and then  $\tilde{x}_{leak_i}(k)$  was calculated. Figure 8 shows the bounds just defined to be adequate for the detection of the leak. Recall that the leakage occurred at  $t_{leak} = 12h$  with its influence being felt at  $t_{leak_i} = 12h00'20''$ . Detection was done at  $t_i = 12h12'$ . So, it took  $11'40''$  to be detected.

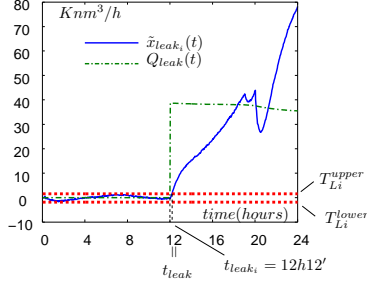


Fig. 8. Leak detection using the intake node pressure as scheduling signal.

To obtain the offtake pressure leakage detector, as we follow exactly the same procedure as for the intake pressure leakage detector, a leakage has been simulated in equal conditions. Its influence was felt at  $t_{leak_o} = 12h00'40''$ . Detection was done at  $t_o = 12h10'$ . The detector took  $9'20''$  to find the leak (see Figure 9).

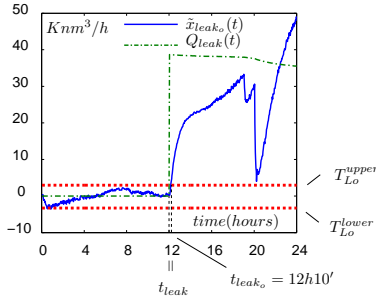


Fig. 9. Leak detection using the offtake node pressure as scheduling signal.

The difference between the time instants,  $t_{leak_i}$  and  $t_{leak_o}$ , when the endpoints pressures begin to drop due to a leak, is a linear function of the leak location. However, this does not coincide with  $t_i - t_o$  due to factors such as noise and the different filters dynamics. As the leakage location is not a known function of the  $t_i - t_o$ , we need more accurate measures of  $t_{leak_i} - t_{leak_o}$  to locate a leakage. This will be done in the next section where an interactive methodology for leakage location is proposed.

## 5. LEAKAGE LOCATION

Figures 8 and 9 show that the signals  $\tilde{x}_{leak_i}(k)$  and  $\tilde{x}_{leak_o}(k)$  are smooth before the leakage is detected and a sudden change occurs with the signal becoming more variable once the leakage is perceived. The idea is to use this variation to estimate  $t_{leak_i}$  and  $t_{leak_o}$ . This sudden change causes a pulse at each differential signal:

$$\begin{aligned}\delta\tilde{x}_{leak_i}(k) &= \tilde{x}_{leak_i}(k) - \tilde{x}_{leak_i}(k-1) \\ \delta\tilde{x}_{leak_o}(k) &= \tilde{x}_{leak_o}(k) - \tilde{x}_{leak_o}(k-1).\end{aligned}$$

From the left frame of Figure 10, we notice that this pulse is masked by the measurement noise. However the same

pulse is perceptible in the right frame of Figure 10, since

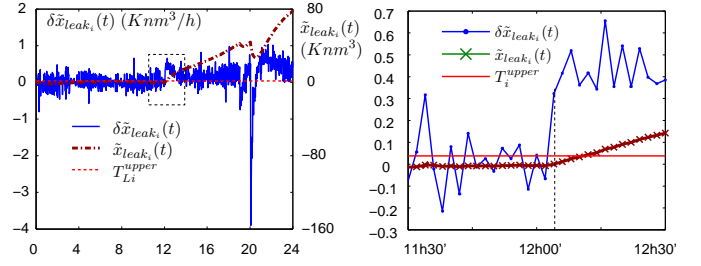


Fig. 10. Left:  $\tilde{x}_{leak_i}(t)$  and its  $\delta\tilde{x}_{leak_i}(t)$ . Right:  $\tilde{x}_{leak_i}(t)$  and its  $\delta\tilde{x}_{leak_i}(t)$  near the time instant where the leak occurs.

this is a magnification of the left frame around the instance that the leakage occurs. Here, a jump in  $\delta\tilde{x}_{leak_i}(k)$  is clear. To detect the leakage, we define a threshold:

$$T_{\delta_i} = \delta M_i + 2\delta\sigma_i$$

where  $\delta M_i$  e  $2\delta\sigma_i$  are, respectively, the expected value and the standard deviation of  $\delta\tilde{x}_{leak_i}(t)$  before the leak is detected. The following values were obtained for these parameters:  $\delta M_i = -0.0011$ ,  $\delta\sigma_i = 0.1608$  and  $T_{\delta_i} = 0.3206$ . From the observation of Figure 10 one may expect a considerable number of false alarms whenever this threshold is adopted. This is confirmed by Figure 11 where the leakage alarms are shown (the red vertical lines).

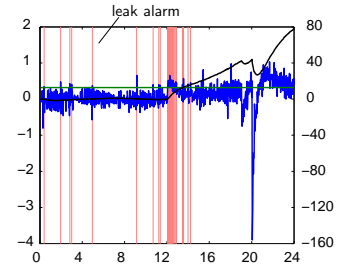


Fig. 11. Leak alarms triggered by  $\delta\tilde{x}_{leak_i}(t)$ .

One may also observe that the density of such points increases significantly immediately before  $\tilde{x}_{leak_i}(t)$  overtakes the leakage detection threshold. Consequently, we may select the first of these points as the first instant that the leakage is perceived by the intake node. That is  $\hat{t}_{leak_i} = 12h04'$ , and this is exactly the sampling instant after the leakage is perceived by the intake pressure.

An identical procedure has been adopted to find the first instant at which the leakage is perceived by the offtake pressure. The following values correspond to the expected value and standard deviation of  $\delta\tilde{x}_{leak_o}(k)$ , respectively:  $\delta M_o = -0.0019$ ,  $\delta\sigma_o = 0.2540$  and  $T_{\delta_o} = 0.3206$  and these values lead to the threshold  $T_{\delta_o} = 0.5061$ .

Figure 12 shows the leakage marks obtained from  $\delta\tilde{x}_{leak_o}(k)$ , which are also more dense immediately before the leakage is detected by the signal  $\tilde{x}_{leak_o}(k)$ . Four false alarms were registered before this sequence started at instant  $\hat{t}_{leak_o} = 12h06'$ , i.e., the instant immediately after the leakage is perceived by the offtake pressure.

Consider now  $x$  the distance from the leakage to the intake node,  $L$  the length of the pipe and  $c$  the speed of the

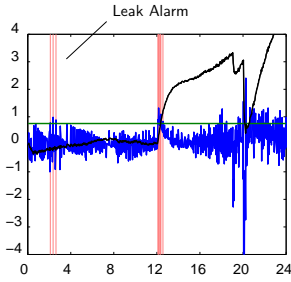
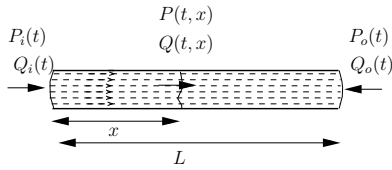


Fig. 12. Leak alarms triggered by  $\delta\tilde{x}_{leak_o}(t)$ .

wave pressure. The wave pressure caused by the leakage takes  $t_{leak_i} = \frac{x}{c}$  sec to be felt by the intake node and  $t_{leak_o} = \frac{L-x}{c}$  sec to be felt by the offtake node.



As  $t_{leak_o} - t_{leak_i} = t_o - t_i = 2' = 120$  sec and  $c = 300$  m/s then  $x = 0$ . This means that the leakage took place at the intake node. As a matter of fact, the leakage happens at  $x = 12$  km! However as a sampling period of 120 sec is the time it takes for a pressure wave to cross 36 Km, the better available resolution is 18 Km. In order to achieve better resolutions, a finer sampling period is required. This is not viable due to technical/equipment limitations at REN-Gasodutos.

## 6. CONCLUSIONS

In this paper, starting from an LPV identification model, first a differential Kalman filter leakage detector is proposed, were two identical detectors are run simultaneously. One considers the scheduling signal as the intake pressure and the other the offtake pressure. When these two detectors run simultaneously a location procedure becomes possible, since the leak location is a linear function of the difference between the time instants the leak is perceived at the pipe endpoints. Based on this fact, an interactive methodology for leakage location has also been presented.

The methodology has been tested with data supplied by REN-Gasodutos, however accuracy of the leakage locator was limited by the long sampling periods possible at REN. The application of the same methodology to more complex pipelines will be considered in the near future with higher sampling rates.

## 7. ACNOWLEDGMENTS

This work was supported in part by FCT, Fundação para a Ciência e Tecnologia.

## REFERENCES

H. Baptista, G. Wagner, and W. Bernhard. Hydraulic model based gas leak detection and location. In *7th Global Congress on Information and Communication Technology in Energy*, 2005.

A. Benkherouf and A. Y. Allidina. Leak detection and location in gas pipelines. *IEEE Proceedings*, 135(2):142–148, March 1988.

P. Lopes dos Santos, T-P Azevedo Perdicoulis, G. Jank, J. A. Ramos, and J. L. Martins de Carvalho. Derivation of a transfer function model for a high pressure pipeline. Technical Report arXiv:1003.5493v1, arXiv, <http://arxiv.org/abs/1003.5493v1>, 04 2010a.

P. Lopes dos Santos, T-P Azevedo Perdicoulis, G. Jank, J. A. Ramos, J. L. Martins de Carvalho, and J. Milhinhos. Modelling a leakage in a high pressure gas network using a quadrupole approach. In *10th Simone Congress, 2010*, 2010b.

G. Geiger and T. Werner. Leak detection and location—a survey. In *PSIG Annual Meeting*, Bern, Switzerland, October 2003.

LIWACOM Informationstechnik GmbH and SIMONE Research Group s.r.o. Simone software: Equations and methods. Technical report, LIWACOM Informationstechnik GmbH and SIMONE Research Group s.r.o., 2004.

M. Liu, S. Zang, and D. Zhou. Fast leak detection and location of gas pipelines based on an adaptive particle filter. *Int. J. Appl. Math. Comput. Sci.*, 15(4):541–550, 2005.

P. Lopes dos Santos, J. A. Ramos, and J. L. Martins de Carvalho. Identification of linear parameter varying systems using an iterative deterministic-stochastic subspace approach. In *European Control Conference ECC-2007*, pages 4867–4873, Kos, Greece, July 2007.

P. Lopes dos Santos, J. A. Ramos, and J. L. Martins de Carvalho. Identification of lpv systems using successive approximations. In *47th IEEE Conference on Decision and Control*, pages 4509–4515, Cancun, Mexico, December 2008a.

P. Lopes dos Santos, J. A. Ramos, and J. L. Martins de Carvalho. Subspace identification of linear parameter varying systems with innovation-type noise model driven by general inputs and a measurable white noise time varying parameter vector. *International Journal of Systems Science*, 39(9):897–911, September 2008b.

P. Lopes dos Santos, J. A. Ramos, and J. L. Martins de Carvalho. Identification of bilinear systems with white noise inputs: an iterative deterministic-stochastic subspace approach. *IEEE Transactions on Control Systems Technology*, 17(3), May 2009.

P. Lopes dos Santos, T-P Azevedo Perdicoulis, G. Jank, J. A. Ramos, J. L. Martins de Carvalho, and J. Milhinhos. Gas pipelines lpv modelling and identification for leakage detection. In *2010 American Control Conference - ACC2010*, 2010.

P. Lopes dos Santos, T-P Azevedo Perdicoulis, G. Jank, J. A. Ramos, J. L. Martins de Carvalho, and J. Milhinhos. An lpv modelling and identification approach to leakage detection in high pressure natural gas transportation networks. *IEEE Transactions on Control Systems Technology*, Special Issue(Waiting publication), January 2011.

Y. Sivathanu. Natural gas leak detection in pipelines, a technology status. Technical report, U. S. Department of Energy, National Energy Technology Laboratory, 2004.

Z. Vostrý. New leak detection and localisation method. In *PSIG Annual Meeting*, Palm Springs, California, USA,

10 2004.

- G. Wagner. Leak sensistivity report, gas transmission system of transgás s.a. Technical report, LIWACOM Informationstechnik GmbH, 2004.
- J. Zhang. Designing a cost effective and reliable pipeline leak detection system. In *Pipeline Reliability Conference*, Houston, USA, 11 1996.